

Efficient Incremental Penetration Depth Estimation between Convex Geometries

Wei Gao

Abstract—Penetration depth (PD) is essential for robotics due to its extensive applications in dynamic simulation, motion planning, haptic rendering, etc. The Expanding Polytope Algorithm (EPA) is the de facto standard for this problem, which estimates PD by expanding an inner polyhedral approximation of an implicit set. In this paper, we propose a novel optimization-based algorithm that incrementally estimates minimum penetration depth and its direction. One major advantage of our method is that it can be warm-started by exploiting the spatial and temporal coherence, which emerges naturally in many robotic applications (e.g., the temporal coherence between adjacent simulation time knots). As a result, our algorithm achieves substantial speedup — we demonstrate it is 5-30x faster than EPA on several benchmarks. Moreover, our approach is built upon the same implicit geometry representation as EPA, which enables easy integration and deployment into existing software stacks. We also provide an open-source implementation for further evaluations and experiments.

I. INTRODUCTION

Penetration depth (PD) is a distance measure that characterizes how much two overlapping shapes penetrate into each other. This distance measure is of significant importance to various robotic applications. For instance, 1) in dynamic simulations, PD is used to calculate the contact force [20], [15], [18] in nearly all rigid body contact models; 2) in motion planning, many planners [19], [17], [9] are designed to regulate (minimize) the PD to alleviate and avoid collisions; and 3) in haptic rendering [7], [13], [11], PD is used to resolve the interactions between objects. PD estimation is usually coupled with binary collision detection, which provides overlapping shape pairs as the input [2], [16]. A common strategy to accelerate collision detection and PD estimation is to split the computation into two phases, as described in [4]. The first phase is the broad phase which eliminates shape pairs that are too distant. The second “narrow” phase checks if the shape pairs passed the broad phase are really colliding, and computes the PD for the colliding pairs. This paper focuses on PD estimation during the narrow phase, as detailed below.

Problem Formulation. We investigate two closed convex shapes $A_1, A_2 \subset R^n$. Usually, the space dimension $n = 2$ or $n = 3$, corresponds to 2-dimensional (2D) or 3-dimensional (3D) setups. Non-convex shapes can be handled by computing their convex-hull [14] or performing convex decomposition [12]. Two shapes A_1, A_2 collide with each other if $A_1 \cap A_2 \neq \emptyset$. For two shapes A_1, A_2 that are in collision, the penetration depth $PD(A_1, A_2)$ between A_1 and A_2 can

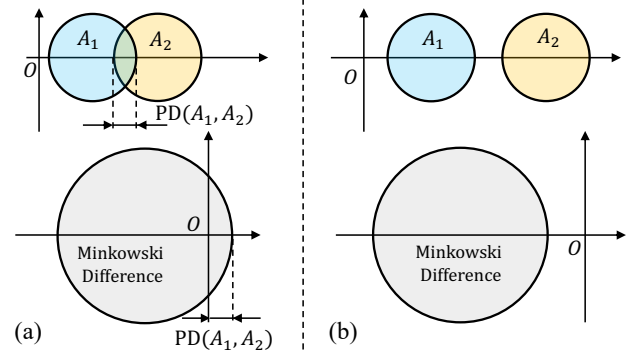


Fig. 1: An illustration of penetration depth and Minkowski Difference. (a) For two colliding shapes, their Minkowski Difference contains the origin O . The penetration depth $PD(A_1, A_2)$ is also the minimum distance from the origin O to the boundary of their Minkowski Difference. (b) For two non-overlapping shapes, the origin O is outside their Minkowski Difference and the penetration depth is not defined.

be define as

$$PD(A_1, A_2) = \min_{d_{1,2} \in R^n} \|d_{1,2}\|_2 \quad (1)$$

subject to: $\text{interior}(A_1 + d_{1,2}) \cap A_2 = \emptyset$

where $\|\cdot\|_2$ is Euclidian norm in R^n ; $A_1 + d_{1,2}$ is the set obtained by applying a displacement $d_{1,2} \in R^n$ to each point in A_1 . The displacement $d_{1,2}^* \in R^n$ that is an optimal solution to Problem (1) is denoted as *minimum penetration displacement*. The unit vector $n_{1,2}^* = \text{normalized}(d_{1,2}^*)$ is usually denoted as *minimum penetration direction*. Obviously, $d_{1,2}^* = n_{1,2}^* \times PD(A_1, A_2)$. An illustration is shown in Fig 1.

Related Works. The most widely used method for PD estimation is the EPA algorithm [21], which is tightly coupled with the Gilbert-Johnson-Keerthi (GJK) algorithm [6] for collision detection. Both GJK and EPA operate on *Minkowski Difference* [6], which is a convex set in R^2 or R^3 constructed from the original shapes A_1 and A_2 (a detailed explanation of Minkowski Difference is presented in Sec. II). Intuitively, the EPA algorithm estimates the PD by building an inner convex polyhedral approximation of the Minkowski Difference. The EPA algorithm requires a tetrahedron inscribed to the Minkowski Difference as the input, which is produced by the GJK algorithm for each colliding shape pair A_1 and A_2 . By using the Minkowski Difference formulation, GJK and EPA can handle many different convex shapes such as convex polyhedra and basic primitives (*i.e.*, spheres, boxes, cylinders etc.). These desirable properties make EPA the de facto standard for PD estimation. On the other hand, an

accurate PD estimation using EPA may require an inner polyhedral approximation with a lot of vertices and faces. In this paper, we take a different approach that incrementally estimates PD by solving an optimization problem. A key advantage of our method is to leverage spatial and temporal coherence in many robotic applications to warm-start the optimization procedure. For instance, in dynamic simulation the object pairs tend to have very similar penetration direction and depth in consecutive simulation steps. Initializing the proposed PD algorithm by the penetration direction of the previous time knot might lead to substantial speed up.

The idea of incrementally estimating the PD has also been explored in [10], which seeks a locally optimal solution of PD by walking on vertices of Gauss maps. However, [10] is restricted to convex polyhedra. As a result, [10] cannot handle general convex geometries and the integration into existing software stacks [2], [16] can be hard. Researchers have also proposed to explicitly construct the Minkowski Difference [3] for collision detection and PD estimation. However, the construction procedures tend to be expensive in terms of memory and computation.

Contributions. Built upon the seminal works [6], [21], [8], this paper proposes a novel PD estimation algorithm between general convex shapes. In particular,

- We formulate PD estimation as a “Difference-of-Convex” problem, which is usually solved by Sequential Quadratic Programming (SQP) [1]. The major challenge of applying SQP to PD estimation is the implicit geometry representation (the *Support Function* explained in Sec. II-B). To address it, we propose a novel instantiation of SQP that utilizes a modified Minkowski Portal Refinement (MPR) algorithm [8] as a subroutine.
- We propose a novel shortcut mechanism that reduces the computation of the vanilla SQP procedure for PD estimation. Furthermore, we demonstrate that the algorithm can still converge to locally optimal solutions despite incorporating the shortcut.
- We experimentally evaluate our method on several benchmarks. Our method demonstrates a 5-30x speedup over EPA at a comparable accuracy.
- We provide an open-source implementation to reproduce the proposed algorithm and facilitate its usage in other robotic applications.

This paper is organized as follows: in Sec. II we introduce the preliminaries about the support function, Minkowski Difference, and MPR algorithm. Sec. III introduces the optimization-based PD algorithm and the shortcut mechanism. Sec. IV presents the experimental results and comparison with the state-of-the-art. Sec. V concludes.

II. PRELIMINARY

A. Minkowski Difference and Penetration Depth

As mentioned in Sec. I, we investigate two closed, convex shapes $A_1, A_2 \subset R^n$. Usually the space dimension $n = 2$ or $n = 3$. The Minkowski Difference $\mathcal{D}_{1,2}$ for shapes A_1 and A_2

is defined as

$$\mathcal{D}_{1,2} = A_1 - A_2 = \{v = v_1 - v_2 | v_1 \in A_1, v_2 \in A_2\} \quad (2)$$

The following properties hold for the Minkowski Difference $\mathcal{D}_{1,2}$:

- $\mathcal{D}_{1,2}$ is a closed convex set if both A_1 and A_2 are closed convex sets.
- Two shapes A_1 and A_2 overlap with each other if the origin $O \in \mathcal{D}_{1,2}$.
- For two overlapping shapes A_1 and A_2 , their penetration depth $\text{PD}(A_1, A_2)$ defined in Problem (1) corresponds to the minimum distance from O to the *boundary* of $\mathcal{D}_{1,2}$, as proved in [21].

An illustration of the Minkowski Difference is provided in Fig. 1. Using these properties, we can reformulate Problem (1) in Sec. I into the following new optimization problem

$$\begin{aligned} \text{PD}(A_1, A_2) = \min_{v \in R^n} \quad & \|v\|_2 \\ \text{subject to:} \quad & v \in \text{boundary}(\mathcal{D}_{1,2}) \end{aligned} \quad (3)$$

Let the point v^* on the boundary of $\mathcal{D}_{1,2}$ be one optimal solution to Problem (4). The minimum penetration displacement $d_{1,2}^*$ in Sec. I can be computed as $d_{1,2}^* = -v^*$. In other words, we have

$$\text{interior}(A_1 - v^*) \cap A_2 = \emptyset \quad (4)$$

The minimum penetration direction in Sec. I can be computed as $n_{1,2}^* = \text{normalized}(-v^*)$.

B. Support Function for Convex Shapes

Explicitly constructing the Minkowski Difference $\mathcal{D}_{1,2}$ can be computationally expensive. Thus, [6] proposed to use an implicit, functional geometry representation called *support function*. For a given convex set A , we can define its support function $\text{supp}_A(\cdot)$ as

$$\text{supp}_A(d) = \text{argmin}_{x \in A} \quad \text{dot}(x, d) \quad (5)$$

where $\text{dot}(\cdot, \cdot)$ is the dot product in R^n , and d is a unit vector denoted as *support direction*. Intuitively, the support function computes points in A that are the farthest along the support direction. For some direction d , there might be more than one point that satisfies the definition in Equ. (5). On the other hand, algorithms in this paper and previous works [6], [21], [8] only need (arbitrary) one such point. Thus, in the following text we assume that the support function $\text{supp}_A(\cdot)$ returns one point for each direction.

The support function is closely related to the *supporting hyperplane* [1] of a convex set. For a given direction d and $v = \text{supp}_A(d)$, the plane $\{x | \text{dot}(d, x - v) = 0\}$ is a supporting plane for the convex shape A at the point $v \in A$. Geometrically, this supporting plane has normal direction d and passes through a point $v \in A$. The convex set A is contained in one of the two closed half-spaces defined by the supporting hyperplane.

As shown in [6], we can use the support functions $\text{supp}_{A_1}(\cdot)$ and $\text{supp}_{A_2}(\cdot)$ of two shapes A_1, A_2 to construct the

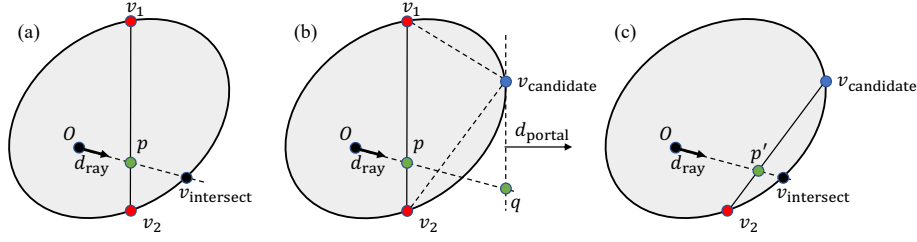


Fig. 2: An illustration of a modified MPR algorithm to compute the intersection point (the $v_{\text{intersect}}$ in (a)) of an origin ray with the boundary of the Minkowski Difference. The algorithm takes the ray direction d_{ray} as the input. In each iteration, the algorithm maintains and updates a “portal”, which is a segment for 2D (or a triangle for 3D) that is inscribed to the Minkowski Difference. The illustrations from (a) to (c) show one MPR iteration, as the portal (v_1, v_2) in (a) is updated to a new portal $(v_2, v_{\text{candidate}})$ in (c). The detailed procedure is explained in Sec. II-C.

support function of their Minkowski Difference $\text{supp}_{\mathcal{D}_{1,2}}(\cdot)$. In particular,

$$\text{supp}_{\mathcal{D}_{1,2}}(d) = \text{supp}_{A_1}(d) - \text{supp}_{A_2}(-d) \quad (6)$$

In other words, we can get a point from $\text{supp}_{\mathcal{D}_{1,2}}(d)$ using the two points from $\text{supp}_{A_1}(d)$ and $\text{supp}_{A_2}(-d)$, respectively. The algorithm presented in this work will access the Minkowski Difference $\mathcal{D}_{1,2}$ through its support function, instead of explicitly constructing it.

C. Minkowski Portal Refinement Algorithm

The MPR [8] algorithm was originally proposed for binary collision checking, in other words determining whether the origin O is contained in the Minkowski Difference $\mathcal{D}_{1,2}$. A brief introduction to a modified MPR is presented, which is used as a subroutine for the algorithm in Sec. III. Please refer to Chapter 7 of [8] for a complete description.

We investigate two overlapping shapes A_1 and A_2 , thus their Minkowski Difference $\mathcal{D}_{1,2}$ contains the origin. Given a direction d_{ray} as the input, we define the *origin ray* that starts from the origin O and extends along d_{ray}

$$\text{origin_ray}(d_{\text{ray}}) = \{x | x = t d_{\text{ray}}, \text{ for } t \geq 0\} \quad (7)$$

We would present a modified MPR algorithm that computes the intersection point of the origin ray with the boundary of Minkowski Difference $\mathcal{D}_{1,2}$, defined as

$$v_{\text{intersect}}(d_{\text{ray}}) = \text{origin_ray}(d_{\text{ray}}) \cap \text{boundary}(\mathcal{D}_{1,2}) \quad (8)$$

An illustration is provided in Fig. 2 (a), and the algorithm is presented in Algorithm 1.

The MPR algorithm maintains and updates a *portal*. As defined in [8], a portal is a n -simplex inscribed to the Minkowski Difference $\mathcal{D}_{1,2} \subset \mathbb{R}^n$ that intersects with the origin ray. For 2D setup ($n = 2$) the portal is a segment inscribed to $\mathcal{D}_{1,2}$. For example, the segment (v_1, v_2) in Fig. 2 (a) is a valid portal that intersects the origin ray at p . In 3D setup ($n = 3$) the portal is a triangle inscribed to $\mathcal{D}_{1,2}$. At the beginning of the algorithm, MPR proposed a “find_portal” procedure [8] to discover a valid portal, as shown in Algorithm 1.

After initialization, MPR first computes the normal of the portal d_{portal} in each iteration, as shown in Fig. 2 and Algorithm 1. Then, the support function is invoked with

Algorithm 1 MPR Algorithm in Sec. II-C

Require: $\mathcal{D}_{1,2}$ with support function $\text{supp}_{\mathcal{D}_{1,2}}(\cdot)$

Require: ray direction d_{ray}

Require: tolerance Δ

portal₀ \leftarrow find_portal($\mathcal{D}_{1,2}$)

while $k = 0, 1, 2, \dots$ **do**

$d_{\text{portal},k} \leftarrow \text{portal_normal}(\text{portal}_k)$

$v_{\text{candidate}} \leftarrow \text{supp}_{\mathcal{D}_{1,2}}(\text{portal}_k)$

$p_k \leftarrow \text{intersect}(\text{origin_ray}(d_{\text{ray}}), d_{\text{portal},k})$

 ▷ A plane is defined by its normal and one point on it

$q_k \leftarrow \text{intersect}(\text{origin_ray}(d_{\text{ray}}), \text{Plane}(d_{\text{portal},k}, v_{\text{candidate}}))$

if $|\text{dot}(q_k - p_k, \text{normalized}(d_{\text{portal},k}))| \leq \Delta$ **then**

return ($p_k, v_{\text{candidate}}, d_{\text{portal},k}$)

end if

 portal_{k+1} \leftarrow update_portal(portal_k, $v_{\text{candidate}}$)

end while

the portal normal to compute a candidate point $v_{\text{candidate}} = \text{supp}_{\mathcal{D}_{1,2}}(d_{\text{portal}})$. As the origin ray intersects with portal (v_1, v_2) , the origin ray must intersect with at least one of the segment $(v_1, v_{\text{candidate}})$ and $(v_2, v_{\text{candidate}})$. The intersecting one will be selected as the new portal for the next iteration. This is the update_portal procedure in Algorithm 1, and the updated portal is $(v_2, v_{\text{candidate}})$ in Fig. 2. The iteration for 3D MPR using triangle portals is conceptually similar, and please refer to Chapter 7 of [8] for a detailed explanation.

It is easy to show the norm $|p| \leq |v_{\text{intersect}}| \leq |q|$, where p, q are the intersecting point of the origin ray with the portal and the supporting hyperplane, as shown in Fig. 2 (b). Thus, one termination condition is to stop the algorithm when the distance between the portal and the supporting hyperplane (at $v_{\text{candidate}}$) is smaller than some tolerance Δ , which can be expressed as $|\text{dot}(q - p, \text{normalized}(d_{\text{portal}}))| \leq \Delta$. Algorithm 1 returns several terms upon convergence, their usage will be introduced in Sec. III-B.

III. PENETRATION DEPTH ESTIMATION ALGORITHM

From the analysis in Sec. II, PD estimation can be expressed in the following optimization problem

$$\begin{aligned} \min_{v \in \mathbb{R}^n} \quad & \|v\|_2 \\ \text{subject to: } \quad & v \in \text{boundary}(\mathcal{D}) \end{aligned} \quad (9)$$

where \mathcal{D} is the Minkowski Difference. Here we drop the subscript of $\mathcal{D}_{1,2}$ for notational simplicity. From the analysis in Sec. II, \mathcal{D} is a closed convex set that contains the origin.

As explained in Sec. II-A, we can only access the convex set \mathcal{D} through its support function $\text{supp}_{\mathcal{D}}(\cdot)$. This implicit geometric representation implies:

- 1) For a given point $v \in \text{boundary}(\mathcal{D})$, it is hard to compute a supporting hyperplane of \mathcal{D} (or equivalently the hyperplane *normal*) that passes through v . This operation is required for many optimization procedures, such as the SQP in Sec. III-A.
- 2) The support function $\text{supp}_{\mathcal{D}}(\cdot)$ is actually an “inverse” of the operation in 1): for a given normal direction d , we can compute a point $v = \text{supp}_{\mathcal{D}}(d)$. This point, combined with the normal d , is able to define a supporting hyperplane for \mathcal{D} .

In this section we will address this challenge and propose an optimization-based PD estimation algorithm.

To make a clear presentation, we will first introduce two “conceptual” algorithms in Sec. III-A and Sec. III-B. The first one highlights the Difference-of-Convex formulation and SQP procedure while assuming we can explicitly compute a supporting hyperplane for any vertex $v \in \text{boundary}(\mathcal{D})$. As mentioned above, this assumption is not true for the Minkowski Difference. To address it, we propose a novel instantiation of SQP that utilizes a modified MPR algorithm as a subroutine. This is the second “conceptual” algorithm in Sec. III-B. Finally, in Sec. III-C we present the actual PD algorithm with a shortcut mechanism. This shortcut can reduce the computation and eliminate the intermediate tolerance parameter for the MPR subroutine in Sec. III-B.

A. Formulation as a Difference-of-Convex Problem

In this subsection, we investigate the following optimization problem, which is very similar to Problem (9):

$$\begin{aligned} \min_{v \in R^n} \quad & \|v\|_2 \\ \text{subject to: } & v \in \text{boundary}(\mathcal{E}) \end{aligned} \quad (10)$$

where \mathcal{E} is also a closed convex set in R^n that contains the origin. Different from Problem (9), we assume an explicit representation of \mathcal{E} is available, such that we can compute a supporting hyperplane for each point $v \in \text{boundary}(\mathcal{E})$. As this assumption does not hold for the Minkowski Difference \mathcal{D} , the PD algorithm presented in this subsection is “conceptual” and will be instantiated in the following subsections.

As a concrete example, the convex shape \mathcal{E} might be represented as the level-set of a continuous convex function $g(v)$. In other words, $\mathcal{E} = \{v | g(v) \leq 0\}$ and $\text{boundary}(\mathcal{E}) = \{v | g(v) = 0\}$. For a point $v \in \text{boundary}(\mathcal{E})$, we can compute a supporting hyperplane whose normal is $-\nabla g(v)$, where ∇ is the subgradient operator.

The domain for the decision variable in Problem (10) only includes the boundary of \mathcal{E} . As the convex set \mathcal{E} contains the origin, we can enlarge the input domain to everywhere

Algorithm 2 SQP for Problem. 11

Require: \mathcal{E} that supports `compute_supporting_hyperplane(\cdot)`

Require: $v_{\text{init}} \in \text{boundary}(\mathcal{E})$

$v_0 \leftarrow v_{\text{init}}$

while $k = 0, 1, 2, \dots$ **do**

$n_{\text{plane},k} \leftarrow \text{compute_supporting_hyperplane}(\mathcal{E}, v_k)$

\triangleright Plane defined by normal $n_{\text{plane},k}$ and a point v_k on it

$y_k \leftarrow \text{project_point_to_plane}(O, \text{Plane}(v_k, n_{\text{plane},k}))$

$v_{k+1} = \text{boundary_intersection}(O_to_y_k, \text{boundary}(\mathcal{E}))$

end while

return v_k

except the inner of \mathcal{E} and rewrite the optimization as

$$\begin{aligned} \min_{v \in R^n} \quad & \|v\|_2 \\ \text{subject to: } & v \in (R^n \setminus \text{inner}(\mathcal{E})) \end{aligned} \quad (11)$$

where $R^n \setminus \text{inner}(\mathcal{E})$ is the complement of $\text{inner}(\mathcal{E})$. Problem (11) can be solved using the Sequential Quadratic Programming (SQP) [1] algorithm, which alternates between linearization of constraints and internal Quadratic Programming (QP) sub-steps. Moreover, Problem (11) is actually a Difference-of-Convex problem. Thus, several additional properties can be used to simplify the SQP:

- SQP usually requires a *trust region*. This trust region can be infinity for Difference-of-Convex problems [1].
- The linearization of the constraint $v \in (R^n \setminus \text{inner}(\mathcal{E}))$ is a halfspace outside the supporting hyperplane. Thus, the inner QP step can be implemented by projecting the origin onto the supporting hyperplane.

The SQP algorithm is presented in Algorithm 2, and the detailed derivation is provided in the Supplemental Material.

As shown in Algorithm 2, the algorithm requires an initial point v_{init} on the boundary of \mathcal{E} . In each iteration, the supporting hyperplane (normal) is first computed. Then, the origin O is projected to the supporting hyperplane to get the point y_k . The point v_{k+1} for the next iteration is computed as the intersection of segment (O, y_k) with $\text{boundary}(\mathcal{E})$. As shown in Supplemental Materials, $|v_k|$ is an upper bound of the penetration depth and it monotonically decreases with iterations ($|v_{k+1}| \leq |v_k|$).

Algorithm 2 cannot be directly applied to Minkowski Difference \mathcal{D} , as it requires explicit geometric representation to compute a supporting hyperplane for each boundary point. This challenge will be addressed in Sec. III-B.

B. Instantiation using MPR as a Subroutine

In this subsection, we adopt the SQP procedure in Algorithm 2 to the Minkowski Difference \mathcal{D} , which is represented by its support function $\text{supp}_{\mathcal{D}}(\cdot)$. For each $v \in \text{boundary}(\mathcal{D})$, we can compute its direction $d_v = \text{normalized}(v)$ and a scalar norm $|v|$. We propose to use d_v as the decision variable and represent v in Problem (11) implicitly by d_v , based on the following observations:

- 1) The point $v \in \text{boundary}(\mathcal{D})$ can be estimated from d_v (with accuracy up on some tolerance Δ), using the MPR algorithm in Sec. II-C as a subroutine.

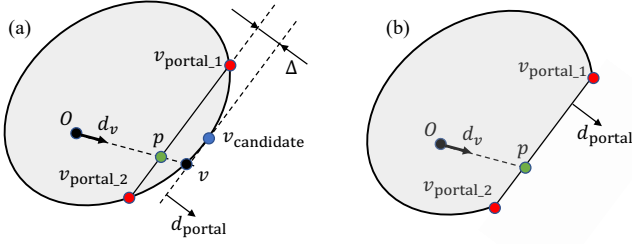


Fig. 3: Approximation scheme used in Sec. III-B and Algorithm 3. (a) shows the configuration of the portal and supporting hyperplane upon the convergence (with tolerance Δ) of MPR, when it is used as a subroutine in Algorithm 3. Intuitively, the approximation in Sec. III-B corresponds to removing all points “outside” the final portal, as shown in (b). A detailed explanation is in Sec. III-B.

- 2) More importantly, the supporting hyperplane normal at v can be approximated by the portal normal d_{portal} , upon the convergence of the MPR algorithm. It is emphasized that usually $d_{\text{portal}} \neq d_v$.

With these observations, we can propose the SQP procedure in Algorithm 3 for the Minkowski Difference \mathcal{D} . The iteration is similar to the one in Algorithm 2. As this algorithm will be superseded in Sec. III-C with a new one with a “shortcut” mechanism, we only provide an intuitive analysis in this subsection.

A critical property of Algorithm 3 is approximating a supporting hyperplane normal by $d_{\text{portal},k}$, which is further illustrated in Fig. 3. Upon the convergence of MPR (Algorithm 1) subroutine with tolerance Δ , the grounding-truth intersecting point v for direction d_v must lie in the between of the portal (segment $(v_{\text{portal}_1}, v_{\text{portal}_2})$ in Fig. 3) and the supporting hyperplane at $v_{\text{candidate}}$. The portal and supporting hyperplane are parallel to each other (they share the same normal d_{portal}), and the distance between these two planes is no more than Δ as the MPR terminates in this iteration. Algorithm 1 uses p to approximate v and uses d_{portal} to approximate a supporting hyperplane normal at v . This approximation is equivalent to removing points from \mathcal{D} that are separated from the origin by the portal, as illustrated in Fig. 3 (b). This is because p is the exact intersecting point for the shape in Fig. 3 (b), while d_{portal} is the exact supporting hyperplane at that intersecting point. The removed part is a convex region whose “thickness” along d_{portal} is no more than Δ . Thus, the approximation becomes more accurate as the tolerance Δ is set smaller.

Despite Algorithm 3 might work in practice, it is not the optimal choice. There can be many iterations in the MPR subroutine for a small tolerance Δ , which is computationally expensive. This issue will be addressed in Sec. III-C.

C. Penetration Depth Estimation with Shortcut

In existing software stacks [16], [2], MPR is typically used with a rather small tolerance to achieve better accuracy. On the other hand, the primary functionality for the MPR subroutine in Algorithm 3 is to produce a search direction d_{k+1} via the supporting hyperplane normal d_{portal} . Thus, we propose to reduce the MPR subroutine iterations by an

Algorithm 3 SQP using Support Function

Require: support function $\text{supp}_{\mathcal{D}}(\cdot)$

Require: initial direction d_{init}

Require: tolerance Δ for MPR subroutine

```

 $d_0 \leftarrow d_{\text{init}}$ 
while  $k = 0, 1, 2, \dots$  do
     $\text{mpr\_output} \leftarrow \text{mpr}(\text{supp}_{\mathcal{D}}, d_k, \Delta)$  ▷ Alg. 1
     $(p_k, v_{\text{candidate}}, d_{\text{portal},k}) \leftarrow \text{mpr\_output}$ 
     $z_k \leftarrow \text{project\_origin\_to\_plane}(\text{Plane}(v_{\text{candidate}}, d_{\text{portal},k}))$ 
    if  $\text{should\_terminate}(p_k, z_k, d_{\text{portal},k})$  then
        return  $z_k$  ▷ Sec. III-D
    end if
     $d_{k+1} \leftarrow d_{\text{portal},k}$ 
end while
return  $p_k$ 

```

early termination mechanism (shortcut) once a “good” search direction is discovered.

Fig. 4 shows the configuration of the portal and the supporting hyperplane configuration in the MPR subroutine. The distance between the portal and the supporting hyperplane might be (much) larger than the tolerance Δ , as it is not necessarily the final iteration. Let the point p be the intersection of $\text{origin_ray}(d_v)$ with the portal. MPR subroutine uses p as the current estimation of v (the intersection with the boundary of \mathcal{D}), and $|p| \leq |v|$. In other words, the PD we would find is *lower* bounded by $|p|$ if we continue the MPR subroutine with direction d_v .

Besides, we can project origin O to the supporting hyperplane to get z , as shown in Fig. 4. Let v_z be the intersection of segment (O, z) with the boundary of \mathcal{D} . Obviously $|v_z| \leq |z|$. If we switch to a new search direction $d_z = \text{normalized}(z)$, the PD we would find is *upper* bounded by $|z|$.

From the analysis above, in each MPR subroutine iteration, we have: 1) a lower bound of PD $|p|$ along the current search direction d_v ; and 2) a new search direction d_z candidate with an upper bound on PD $|z|$ along it. We propose to switch to the new search direction d_z once the upper bound along it is smaller than the lower bound along the original direction d_v , as shown in Fig. 4.

With the analysis above, the overall PD estimation algorithm is summarized in Algorithm 4, which uses a subroutine in Algorithm 5. The SQP procedure is almost identical to Algorithm 3, except that the MPR subroutine is changed to Algorithm 5. The MPR subroutine would be terminated early with the abovementioned condition, as shown in Algorithm 5. Despite the new shortcut mechanism, this SQP is guaranteed to converge to a locally optimal solution. Please refer to the Supplemental Material for a detailed analysis.

D. Implementation Details

Initialization. As shown in Algorithm 4, the SQP procedure requires an initial direction d_{init} as the input. This is a guess of the smallest displacement direction that could move shape A_1 away from colliding with shape A_2 . For applications that

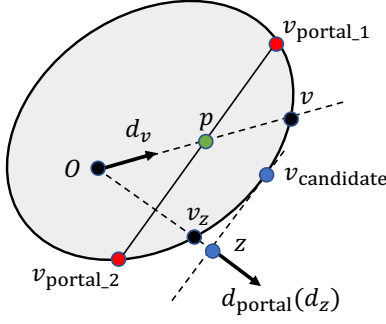


Fig. 4: An illustration of the shortcut mechanism in Sec. III-C. The penetration depth along d_v is lower bounded by $|p|$, while the penetration depth along $d_{\text{portal}}(d_z)$ is upper bounded by z . We proposed to switch to d_z as the new search direction when $|p| \geq |z|$, as explained in Sec. III-C.

Algorithm 4 Proposed SQP Algorithm for PD Estimation

Require: support function $\text{supp}_{\mathcal{D}}(\cdot)$

Require: initial direction d_{init}

Replaces the invoked MPR subroutine in Algorithm 3 by `mpr_shortcut` in Algorithm 5. The tolerance Δ in Algorithm 3 is no longer necessary.

exhibit high spatial or temporal coherence between successive frames/time-knots, there might be a good application-specific guess of the minimum penetration direction. For instance, in dynamic simulation [20], [15], [18] colliding object pairs tend to have very similar penetration direction and depth in consecutive simulation steps. Similarly, in optimization-based motion planning [19], [17], [9] we might use the penetration direction from the previous optimization iteration as d_{init} , especially for planning algorithms with trust-region mechanisms to ensure a small difference between consecutive iterations.

If application-specific prior about penetration direction is unavailable, one alternative method is to use the centroid difference between two shapes as d_{init} . The original MPR [8] implemented in existing software stacks [16], [2] also requires the centroid of shapes (although an inner point is sufficient for the algorithm). Thus, this initialization scheme can be directly plugged in with minimal engineering effort.

Termination and Result. As the PD is usually used to resolve the collision in downstream tasks, it is better to overestimate the PD than underestimate it. Thus, the upper bound z_k is returned upon termination in Algorithm 4. A point v on the boundary of \mathcal{D} is the local optima of $|v|$ if v is perpendicular to one supporting hyperplane at v . In this situation, the MPR subroutine cannot find a new direction. Thus, we would terminate the SQP in Algorithm 4 if the new search direction $d_{\text{portal},k}$ is the same as the old one normalized(p_k) up to some tolerance. Moreover, the gap between the lower bound p_k and the upper bound z_k should be rather small under this situation, which is also included in the termination condition.

Algorithm 5 MPR Subroutine with Shortcut in Sec. III-C

Require: $\mathcal{D}_{1,2}$ with support function $\text{supp}_{\mathcal{D}_{1,2}}(\cdot)$

Require: ray direction d_{ray}

$\text{portal}_0 \leftarrow \text{find_portal}(\mathcal{D}_{1,2})$

while $k = 0, 1, 2, \dots$ **do**

$d_{\text{portal},k} \leftarrow \text{portal_normal}(\text{portal}_k)$

$v_{\text{candidate}} \leftarrow \text{supp}_{\mathcal{D}_{1,2}}(\text{portal}_k)$

$p_k \leftarrow \text{intersect}(\text{origin_ray}(d_{\text{ray}}), d_{\text{portal},k})$

\triangleright A plane is defined by its normal and one point on it

$z_k \leftarrow \text{project_origin_to_plane}(\text{Plane}(v_{\text{candidate}}, d_{\text{portal},k}))$

if $|z_k| \leq |p_k|$ **then** \triangleright Shortcut in Sec. III-C

return $p_k, v_{\text{candidate}}, d_{\text{portal},k}$

end if

$\text{portal}_{k+1} \leftarrow \text{update_portal}(\text{portal}_k, v_{\text{candidate}})$

end while

IV. RESULTS

In this section, we experimentally investigate the robustness, accuracy and efficiency of the proposed method. Our method is implemented in a forked `fcl` [16] library. The proposed method is compared with the EPA [21] algorithm in `libccd` [5], a popular library used in various physical engines and collision detectors [16], [18]. Parameters are tuned such that all algorithms have roughly the same accuracy and are fixed for the entire experiment after tuning. Please refer to Supplemental Materials for more details. Our method is evaluated on two sets of shapes. The first one consists of simple primitives, and the second set is convex polyhedra with different numbers of vertices. Our hardware platform is a desktop with AMD 3970x CPU running Ubuntu 20.04. Our implementation is open-sourced at this link.

A. Primitive Shapes

In this subsection, we consider the penetration depth between three types of shape pairs:

- Sphere collides with sphere (sphere vs. sphere)
- Capsule collides with capsule (capsule vs. capsule)
- Sphere collides with capsule (sphere vs. capsule)

For these simple primitive shapes, the `fcl` [16] library provides hand-written algorithms to compute their penetration, which is used as ground truth to evaluate the accuracy of PD algorithms. The geometries have characteristic dimensions (such as the diameter of the sphere) of 1 meter in this experiment. For more details, please refer to the Supplemental Materials. All of the statistical results are the averaged value of 10000 independent runs with randomly generated poses for the shape pair.

Our method requires an initial penetration direction guess. For the purpose of benchmarking, we use the following method to obtain the initial guess. Given the ground truth penetration direction from the hand-written algorithm, we apply a rotation of n degrees with respect to a random axis that is perpendicular to the ground-truth direction. Then, the rotated direction is used as the initial guess.

	Ours (5°)	Ours (25°)	Ours (45°)	EPA
Sphere vs. Sphere	0.909	1.018	1.03	1.58
Capsule vs. Capsule	1.092	1.12	1.12	0.39
Sphere vs. Capsule	1.255	1.31	1.30	1.72

TABLE I: The PD error of various algorithms compared with the ground truth. The result errors are the average of 10000 independent runs expressed in micrometers (10^{-6} meter). Our method is evaluated with different angular deviations (of initial penetration direction) at 5°, 25°, and 45°. Geometries have characteristic dimensions (such as the diameter of the sphere) of 1 meter.

Table. I shows the accuracy of our method under different rotation perturbation angles n , where n ranges from 5° to 45°. We report the average deviation of the estimated PD from the ground truth among 10000 independent runs. From Table I, both EPA and our method can accurately estimate penetration depth. The results from the proposed algorithm can be rather accurate despite the large initialization error. Moreover, all the penetration depths and directions computed by our method lead to the separation of two shapes, as explained in Equ. 1.

Table. II summarizes the performance of our method and the EPA baseline. Our method achieves 20x-30x speed up compared to EPA. Moreover, the performance improvement is consistent for different shape types and deviations of initial guess direction.

B. Convex polyhedra

The second experiment considers the penetration detection estimation involving convex polyhedra. We use the sphere-capsule penetration similar to Sec IV-A, but replace the sphere with its convex polyhedral approximation. This approximation is constructed by discretizing the sphere at different resolutions. Higher resolution with more vertices and faces improves the approximation accuracy at the cost of computational complexity. Please refer to the Supplemental Material for more details. The ground truth penetration is unavailable due to the discretization error.

Fig. 6 shows the performance of the proposed algorithm with respect to the number of vertices in the convex polyhedra. Our method is evaluated with different angular deviations (of initial penetration direction) at 5° and 45°. The proposed method consistently outperforms EPA baselines with about 5-10x speedup.

A comparative experiment is conducted to highlight the benefit of the proposed shortcut mechanism in Sec. III-C. We use an initial direction deviation of 45°, and the result is shown in Fig. 5. The number of support function invocations and running time are used to characterize the performance. From the figure, the proposed shortcut mechanism can halve the required support function invocations and lead to about 2-3x speedup.

	Ours (5°)	Ours (25°)	Ours (45°)	EPA
Sphere vs. Sphere	1.9	2.1	2.3	85.1
Capsule vs. Capsule	1.6	1.9	2.0	39.5
Sphere vs. Capsule	2.0	2.2	2.4	61.5

TABLE II: Performance of the proposed method under different angular deviations of the initial direction guess. Results are the averaged time in microseconds computed from 10000 independent runs with different colliding poses. The proposed method is 20x-30x times faster than EPA.

V. CONCLUSION

In this paper, we contribute a novel algorithm to estimate the PD between convex shapes. To achieve this, we formulate the PD estimation as a Difference-of-Convex optimization. Then, we propose a novel instantiation of SQP using a modified MPR subroutine that solves the optimization-based PD estimation. We further present a shortcut mechanism that significantly reduces the computation. Through various experiments, we show that the proposed method achieves a 5-30x speedup over the well-known EPA algorithm at comparable accuracy. Moreover, the proposed method uses the same support function representation as existing works [6], [21], [8]. Thus, it can be easily integrated into existing software stacks [16], [2]. The source code is provided to facilitate further evaluation and application.

VI. ACKNOWLEDGMENTS

This work was conducted during the author’s employment at Mech-Mind Robotics. The views expressed in this paper are those of the authors themselves and are not endorsed by the supporting agencies.

REFERENCES

- [1] S. Boyd, S. P. Boyd, and L. Vandenberghe. *Convex optimization*. Cambridge university press, 2004.
- [2] E. Coumans and Y. Bai. Pybullet, a python module for physics simulation for games, robotics and machine learning. 2016.
- [3] D. Dobkin, J. Hershberger, D. Kirkpatrick, and S. Suri. Computing the intersection-depth of polyhedra. *Algorithmica*, 9(6):518–533, 1993.
- [4] C. Ericson. *Real-time collision detection*. Crc Press, 2004.
- [5] D. Fiser. Libccd: Library for collision detection between two convex shapes, 2015.
- [6] E. G. Gilbert, D. W. Johnson, and S. S. Keerthi. A fast procedure for computing the distance between complex objects in three-dimensional space. *IEEE Journal on Robotics and Automation*, 4:193–203, 1988.
- [7] A. Gregory, A. Mascarenhas, S. Ehmann, M. Lin, and D. Manocha. Six degree-of-freedom haptic display of polygonal models. In *Proceedings Visualization 2000.*, pages 139–146. IEEE, 2000.
- [8] S. Jacobs. *Game programming gems 7*. 2008.
- [9] D. Kappler, F. Meier, J. Issac, J. Mainprice, C. G. Cifuentes, M. Wüthrich, V. Berenz, S. Schaal, N. Ratliff, and J. Bohg. Real-time perception meets reactive motion generation. *IEEE Robotics and Automation Letters*, 3(3):1864–1871, 2018.
- [10] Y. J. Kim, M. C. Lin, and D. Manocha. Incremental penetration depth estimation between convex polytopes using dual-space expansion. *IEEE transactions on visualization and computer graphics*, 10(2):152–163, 2004.
- [11] V. Kumar and E. Todorov. Mujoco haptix: A virtual reality system for hand manipulation. In *2015 IEEE-RAS 15th International Conference on Humanoid Robots (Humanoids)*, pages 657–663. IEEE, 2015.

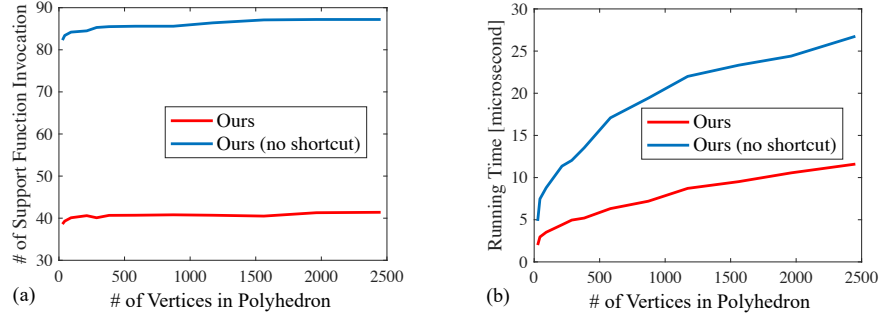


Fig. 5: A comparative experiment is conducted to highlight the benefit of the proposed shortcut mechanism in Sec. III-C. In the figure, (a) shows the performance measured by the number of support function invocations, while (b) shows the performance in microseconds. The proposed shortcut mechanism can halve the required support function invocations and lead to about 2-3x speedup.

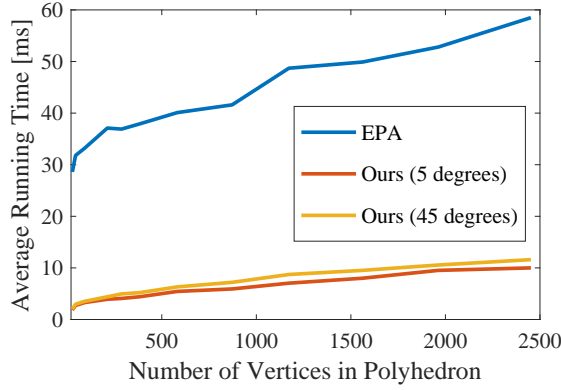


Fig. 6: The performance of various PD algorithms with respect to the number of vertices in convex polyhedron. Results are the averaged time in microseconds computed from 10000 independent runs. Our method is evaluated with different angular deviations (of initial penetration direction) at 5° and 45° . The proposed method achieves substantial speedup compared to the EPA baseline.

- [21] G. Van Den Bergen. Proximity queries and penetration depth computation on 3d game objects. In *Game developers conference*, volume 170, 2001.

- [12] K. Mamou and F. Ghorbel. A simple and efficient approach for 3d mesh approximate convex decomposition. In *2009 16th IEEE international conference on image processing (ICIP)*, pages 3501–3504. IEEE, 2009.
- [13] W. A. McNeely, K. D. Puterbaugh, and J. J. Troy. Six degree-of-freedom haptic rendering using voxel sampling. In *ACM SIGGRAPH 2005 Courses*, pages 42–es. 2005.
- [14] A. A. Melkman. On-line construction of the convex hull of a simple polyline. *Information Processing Letters*, 25(1):11–12, 1987.
- [15] B. Mirtich. Rigid body contact: Collision detection to force computation. In *Workshop on Contact Analysis and Simulation, IEEE Intl. Conference on Robotics and Automation*, 1998.
- [16] J. Pan, S. Chitta, and D. Manocha. Fcl: A general purpose library for collision and proximity queries. In *IEEE International Conference on Robotics and Automation*, pages 3859–3866. IEEE, 2012.
- [17] J. Schulman, J. Ho, A. X. Lee, I. Awwal, H. Bradlow, and P. Abbeel. Finding locally optimal, collision-free trajectories with sequential convex optimization. Citeseer.
- [18] E. Todorov. Convex and analytically-invertible dynamics with contacts and constraints: Theory and implementation in mujoco. In *2014 IEEE International Conference on Robotics and Automation (ICRA)*, pages 6054–6061. IEEE, 2014.
- [19] M. Toussaint, K. Allen, K. A. Smith, and J. B. Tenenbaum. Differentiable physics and stable modes for tool-use and manipulation planning.
- [20] J. C. Trinkle, J.-S. Pang, S. Sudarsky, and G. Lo. On dynamic multi-rigid-body contact problems with coulomb friction. *ZAMM-Journal of Applied Mathematics and Mechanics/Zeitschrift für Angewandte Mathematik und Mechanik*, 77(4):267–279, 1997.